

Adaptive Admittance-based Conductor Meshing for Interconnect Analysis

Abstract— We present a new algorithm for discretizing interconnects, a step that is typically performed to account for the non-uniformity of current flow at high frequencies. The algorithm is based on an easily-computable measure that correlates well with the model accuracy. This measure is used to refine the discretization of interconnects in an adaptive scheme so as to systematically trade off computation against model accuracy. We apply the proposed discretization technique on two classes of problems in the analysis of VLSI interconnects: simulation and frequency-dependent inductance extraction. Numerical results established that with the interconnect discretizations generated by our algorithm, 3 to 7 times reduction in simulation and extraction times can be realized with negligible sacrifice in model accuracy (< 1% errors).

I. INTRODUCTION

The current distribution across modern interconnects is far from uniform owing to two main reasons. The first is the *skin effect* that occurs due to high signal frequencies. For at least the case of a single conductor carrying a signal at a single frequency, the current density $J(x)$ drops off exponentially as a function of the distance x from the conductor surface into the interior: $J(x) = J(0)e^{-x/\delta}$, where δ is the skin depth [1]. The second reason for the non-uniformity of current flow is the *proximity effect*, caused by the presence of nearby conductors. The usual technique to account for skin and proximity effects is to discretize the conductor into filaments, which results in a larger lumped circuit model. The finer the discretization, the more accurate the model; however, this accuracy comes with the high computational cost that is required to manipulate and simulate the high-order model.

Perhaps the simplest discretization scheme is the *uniform meshing* (UM) scheme, where a conductor is discretized so that the filaments are all of the same cross-sectional area, with the width and the height of each filament being no larger than the skin depth δ . However, the skin and proximity effects cause the current flow to crowd at the edges and at the corners. This motivates the *exponential meshing* (EM) where the width and height of filaments increase exponentially from outside to inside [1], with the width and the height of the smallest filament being no larger than the skin depth. The ratio of the width of a filament to a smaller adjacent filament is typically taken as two. Fig. 1 shows the cross-section of conductor with these two meshing schemes.

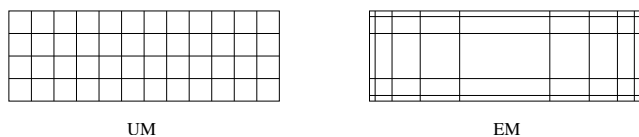


Fig. 1. Meshing of conductor.

A fundamental issue with the UM and EM schemes is where they fit in the context of the accuracy versus computation trade-off. Numerical experiments reveal that both

these schemes perform excellently in terms of model accuracy. Moreover, the EM scheme, as expected, is slightly inferior to the UM scheme, but with a much reduced computational demand. We will establish in this paper that considerable further reduction in computation can be realized with negligible sacrifice to modeling accuracy.

A simple exploration of reducing the computational demand with meshing schemes would proceed as follows: Beginning with any scheme whose accuracy is acceptable, coarsen the discretization until the loss of accuracy is no longer acceptable. The term “accuracy” here refers to the model accuracy, the determination of which typically involves simulation, and is therefore computationally demanding. We will demonstrate in §II the existence of a quantity that is (i) easily computable given any meshing scheme and (ii) correlates very well with the model accuracy. This quantity can thus be used to quickly estimate the model accuracy at a given level of discretization, replacing the costly simulation. This idea forms the heart of the adaptive schemes that we propose in §III and §IV to determine a discretization that maximizes the reduction in computation, yet yielding an acceptable model accuracy. Through an analysis of the complexity of the proposed adaptive meshing schemes, we will establish that the computational overhead is indeed minor. Numerical results in §V demonstrate the superior performance of our technique in the problems of simulation and frequency-dependent inductance extraction.

II. A QUANTITY THAT TRACKS SIMULATION ERROR

To begin, consider a single conductor carrying a signal at a single angular frequency ω . Let $\mathcal{G}_1, \mathcal{G}_2, \dots$ describe a sequence of discretizations with the property that \mathcal{G}_{i+1} is “strictly finer” than \mathcal{G}_i , i.e., every filament in \mathcal{G}_{i+1} is contained in some filament in \mathcal{G}_i , and at least one filament in \mathcal{G}_{i+1} is not contained in any filament in \mathcal{G}_i (see Fig. 2). Moreover, let the largest dimension (width or height) of any filament go to zero with i . Let L_i and R_i be the inductance and resistance matrices with discretization \mathcal{G}_i . Then, with a voltage difference of one Volt between the two terminals, the vector of filament currents I_i at discretization \mathcal{G}_i is given by

$$I_i = (R_i + j\omega L_i)^{-1} \mathbf{1}, \quad (1)$$

where $\mathbf{1}$ denotes a vector of ones. The total current in the conductor $\mathbf{1}^T I_i = \mathbf{1}^T (R_i + j\omega L_i)^{-1} \mathbf{1}$, thus is the conductor-level complex admittance Y_i at discretization \mathcal{G}_i .

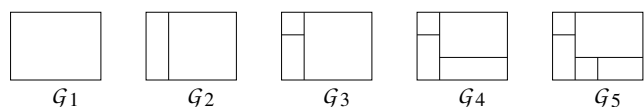


Fig. 2. An example of the sequence of meshing: $(\mathcal{G}_1, \mathcal{G}_2, \mathcal{G}_3, \mathcal{G}_4, \mathcal{G}_5)$.

We first note that $|Y_i|$ is an *increasing* sequence. This follows from physical reasoning, as with increasing i , an increasing

number of current paths are included in the model: The currents of the conductor with discretization \mathcal{G}_i contain all the currents of the conductor with discretization \mathcal{G}_{i-1} , thereby increasing the admittance magnitude. We next note that the sequence $|Y_i|$ converges to the true value of the conductor-level admittance, denoted $|Y_\infty|$. Indeed, the latter observation holds true for *any* sequence of meshing schemes where the discretizations become finer, i.e., when the width and height of the largest filament go to zero. Combining these two observations, we can conclude that the discretization with the higher admittance magnitude is closer to the ideal, and is hence more accurate. Moreover, the admittance magnitude serves as a measure to compare the accuracy of any two discretizations: The admittance error $|Y_\infty| - |Y_i|$ is equal to the steady-state error in the current amplitude when a unit sinusoidal voltage at frequency ω is applied between the terminals of the conductor. These observations provide a straightforward method for determining an acceptable discretization: Begin with a coarse grid, and continue with a sequence of finer grids until $|Y_\infty| - |Y_i|$ is small. However, the quantity $|Y_\infty|$ is seldom available, and even its approximate computation requires manipulation of very large matrices of doubtful conditioning. We now present a simple variant of this idea that circumvents this difficulty.

Instead of the current error (which equals the admittance error $|Y_\infty| - |Y_i|$), consider instead the *change in the current error*, whose magnitude equals $|Y_{i+1}| - |Y_i|$. Intuitively, as the discretization becomes finer, the change in the magnitude of the current error should go to zero; thus, we will use this easily computable quantity to define the stopping criterion of the meshing schemes. Therefore, the basic idea behind much of the development in this paper can be summarized as: “Begin with a coarse grid, and continue with a sequence of finer grids until $|Y_{i+1}| - |Y_i|$ is small.”

The preceding discussion applies to steady-state analysis at a single frequency. We now establish via a simple numerical example that the principles outlined above apply to analysis with more realistic signals as well. Consider a single conductor with cross-section $3 \times 3 \mu\text{m}$ and length $1000 \mu\text{m}$, with a voltage signal that is a 1V ramp with a rise-time of 10ps. Let $\{\mathcal{G}_i\}$ denote a sequence of increasingly fine discretizations with the UM scheme. Figure 3 compares two quantities: The first is the change in the admittance magnitude $|Y_{i+1}| - |Y_i|$ computed at a frequency of 100GHz. The second is the change in the simulation error, defined as $\max(|I(t) - I_i(t)|)$, where $I(t)$ is the “true” current in the conductor (computed with a very fine UM discretization, size 29×29) and $I_i(t)$ the current obtained using SPICE simulations of the UM discretization \mathcal{G}_i . It is evident that the change in the admittance magnitude indeed tracks the change in the simulation error, even for the more commonly ramp waveforms.

III. ADAPTIVE MESHING SCHEMES

Recalling that the current flow typically decreases exponentially into the interior of the conductor, we next consider meshing schemes that retain the principle behind the conventional exponential meshing, yet adaptively try to obtain the coarsest

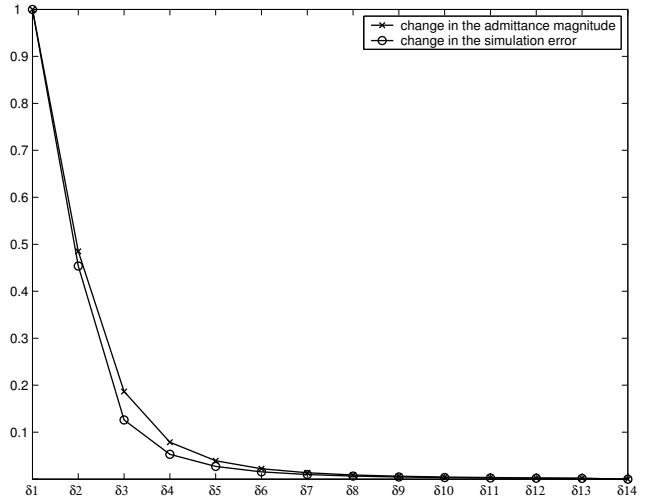


Fig. 3. The change in the admittance magnitude closely tracks the change in the simulation error (“ δi ” denotes the quantity of $|Y_{i+1}| - |Y_i|$).

meshing scheme of acceptable accuracy. For easy reference, we briefly describe two exponential meshing (EM) schemes which we call EM-1 and EM-2.

EM-1 is a popular meshing scheme, described in [1]. We describe the meshing along the width (the meshing along the height proceeds similarly). Given a wire of width w , let N_1 and N_2 be the smallest integers satisfying

$$\frac{w}{2(1 + 2 + 2^2 + \dots + 2^{N_1-1})} \leq \delta,$$

and

$$\frac{w}{2(1 + 2 + 2^2 + \dots + 2^{N_2-2}) + 2^{N_2-1}} \leq \delta.$$

Then, the number of filaments along the width with EM-1 is $\min\{2N_1, 2N_2 - 1\}$. An example of a conductor discretized along its width using the EM-1 scheme is shown in Fig. 4 where $N_2 = 3$ and $\delta' = \frac{w}{2(1 + 2) + 2^2}$.

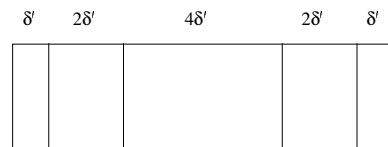


Fig. 4. An example of EM-1.

The feature characterizing EM-1 is that the smallest filament is of width less than or equal to the skin depth, with the filament widths doubling towards the interior. The number of filaments is determined automatically. In contrast, with EM-2, a second exponential meshing scheme [4], the number of filaments is specified a priori. This meshing scheme then holds the smallest filament width at the skin depth, and adjusts the ratio between adjacent filaments so as to fit the filaments inside the given width w . More precisely, given a conductor of width w and N , the number of desired filaments, the ratio r between

adjacent filaments satisfies

$$w = \begin{cases} 2\delta \left(\frac{r^{N/2} - 1}{r - 1} \right), & \text{even } N, \\ 2\delta \left(\frac{r^{(N-1)/2} - 1}{r - 1} \right) + \delta r^{(N-1)/2}, & \text{odd } N. \end{cases} \quad (2)$$

While EM-1 and EM-2 perform excellently in terms of model and simulation accuracy and are widely used in practice, we will show that *significant* savings in computation can be realized with alternate meshing schemes, at *negligible* loss in accuracy. In other words, conventional EM schemes are an over-kill. Instead, we propose two meshing schemes, where the number of filaments is increased until it can be established that additional filaments yield no discernible improvement in accuracy.

The first such scheme that we consider is an *adaptive exponential meshing* scheme, denoted AEM-1. This scheme is inspired by the conventional exponential meshing scheme EM-1. The basic idea is to hold the outermost (smallest) filaments at a width of δ , and begin adding filaments whose widths double towards the interior, until the admittance magnitude does not increase appreciably or when there is no room for adding any more filaments. We note that if the latter happens, AEM-1 is very similar to EM-1; however, we will demonstrate through numerical examples that this is seldom the case; the AEM-1 meshing scheme typically terminates well before the EM-1 limit is reached, accruing considerable computational savings and indicating that the EM-1 scheme over-meshes.

An example of the AEM-1 discretization sequence is shown in Fig. 5. Note that the number of filaments with AEM-1 is almost always odd. Discretization \mathcal{G}_1 has only one filament (i.e., no discretization). Discretization \mathcal{G}_2 has three filaments, with the outermost filaments of width δ , the skin-depth (this assumes that the dimension that is being discretized is of width at least 2δ ; otherwise the meshing scheme terminates with \mathcal{G}_1). If the width is at least 6δ , there exists discretization \mathcal{G}_3 with five filaments, with the outermost filaments of width δ , the next pair of inner filaments of width 2δ , with the middle filament spanning the rest of the width.

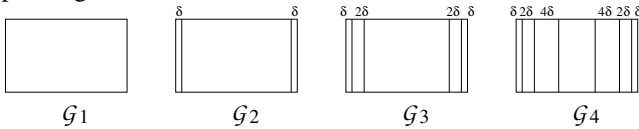


Fig. 5. The discretization sequence of AEM-1.

The second adaptive exponential meshing scheme, denoted AEM-2, is very similar to the conventional exponential meshing scheme EM-2. Here, holding the width of the outermost filaments constant at the skin depth, the number of filaments N is incremented with the ratio r between adjacent filaments satisfying (2), until the admittance magnitude does not increase appreciably. Note that AEM-2 is identical to EM-2 when the number of filaments match; the crucial difference is that with EM-2, the number of filaments is to be specified a priori, whereas with AEM-2, the the number of filaments is adaptively determined.

Fig. 6 illustrates an example of an AEM-2 discretization sequence. As with AEM-1, the number of filaments with AEM-2 is almost always odd. The discretization pattern of \mathcal{G}_1 and \mathcal{G}_2 match those of AEM-1 (see Fig. 5). With discretization \mathcal{G}_3 , there are five filaments, with the outermost filaments of width δ , the next pair of inner filaments of width $r\delta$, and with the middle filament of width $r^2\delta$.

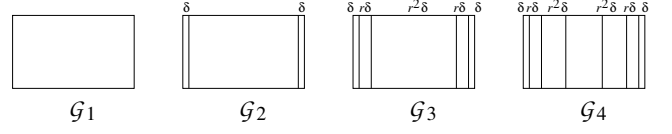


Fig. 6. The discretization sequence of AEM-2.

Recall that in §II (see Fig. 3 in particular), we demonstrated that the change in the admittance magnitude tracks the true simulation error fairly well. We now show that this observation can be used in conjunction with the proposed meshing schemes AEM-1 and AEM-2 to achieve an acceptable modeling and simulation accuracy with far less computation. We will present detailed simulations backing this claim in §V; we give a brief preview here, considering a conductor with the cross-section of $12.6 \times 1.05\mu\text{m}$ and the length of $1000\mu\text{m}$. The different meshing schemes compared are: UM (60×5 grid; this will be taken as the “standard”); EM-1 (10×4); EM-2, also with an 10×4 grid; AEM-1 (5×3 grid); and AEM-2 (5×3 grid) (see Fig. 7). The relative simulation error of the various meshing schemes are presented in Fig. 8 (SPICE was used to perform the numerical simulations). Here, the simulation error is defined as $\max(|I(t) - \hat{I}(t)|)$, where $I(t)$ is the current in the conductor obtained with UM, and $\hat{I}(t)$ the current obtained from one of the four (non-adaptive and adaptive) exponential meshing schemes. The results confirm that the resulting loss in accuracy obtained with the coarser meshes in the AEM-1 and AEM-2 schemes is insignificant. We shall show in §V that the computation required by the AEM schemes is considerably less than that required by the conventional EM schemes.

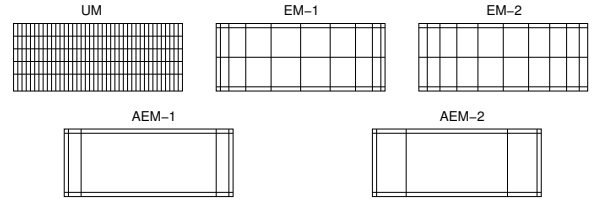


Fig. 7. Various meshing schemes used in the comparative study.

IV. IMPLEMENTATIONS OF ADAPTIVE MESHING SCHEMES

While we have established that it is possible to achieve sufficient modeling accuracy with meshing schemes that are coarser than conventional EM schemes, the question of systematically determining such a coarse mesh remains. The approach that we present uses the following simple steps: Given a discretization that needs refinement, we consider two candidate discretizations, one with two more filaments along the width, and the other with two more filaments along the height. We then compute the admittance magnitude at the working frequency ω , and choose the discretization

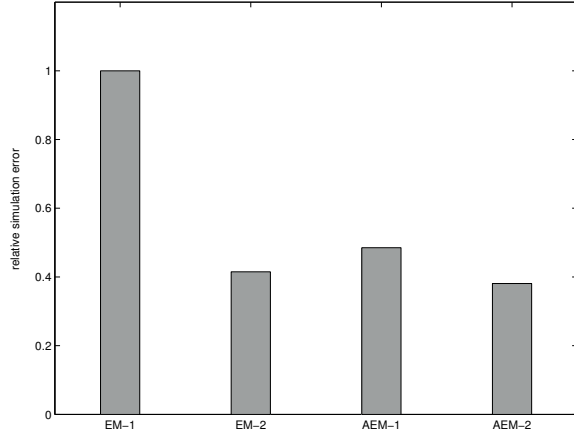


Fig. 8. The relative simulation error of the various meshing schemes.

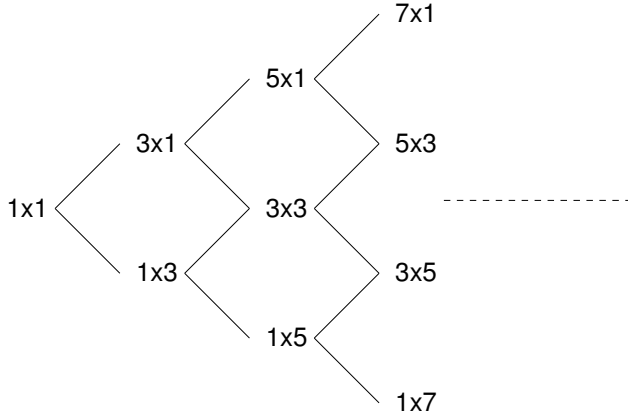


Fig. 9. “Binary” decision diagram of meshing.

that yields a higher admittance magnitude. Beginning with a 1×1 grid, the refinement proceeds along a “binary” decision diagram, shown in Fig. 9, to define a sequence of finer grids. The process stops when the change in the admittance magnitude between two successive discretizations is below a suitably chosen threshold. For example, the admittance values corresponding to the different discretizations in Fig. 9 for a single wire of length 1mm with cross section $10\mu\text{m} \times 3\mu\text{m}$ are shown in Fig. 10. This figure also shows the sequence of discretizations traversed by our algorithm.

The discussion so far has focused on a single conductor, thus addressing the non-uniformity in current flow arising from the skin effect. A natural question is whether proximity effects (i.e., non-uniformity of current flow attributable to the presence of nearby conductors) should be separately accounted for. We now present an intuitive argument that answers this in the negative. (We will also present empirical evidence that backs this claim.) The argument is simply that discretizing a conductor effectively treats a conductor as a bundle of filaments, whose “proximity” effect is indeed the skin effect. As the filaments in bundle are much closer to each other than the filaments from any other conductors, the interaction of the former overwhelm any effects from the latter.

To illustrate the above arguments, consider three conductors all of length 1mm and cross section $10\mu\text{m} \times 3\mu\text{m}$, with the

middle one being the victim that is sandwiched between two “aggressors.” We begin with a discretization of the victim (5×3) that is based on an analysis of its “standalone” admittance magnitude. We then consider its admittance in the presence of the aggressors (which are also discretized using a standalone analysis), and consider the change in this true admittance when the victim is discretized with finer and finer meshing schemes (holding the aggressor discretization constant). Table I shows the current error (obtained via a SPICE variant when the aggressors are triggered by a 1V ramp with a rise-time of 10ps) in the victim for a number of discretizations for the victim, and for a number of values of inter-conductor spacing. It is evident that the current error does not change with finer discretizations of the victim beyond the 5×3 mesh.

Summarizing the above discussions, Fig. 11 illustrates the overall implementation of our technique. Inputs are any single conductor with an initial discretization $\mathcal{G}_{\text{initial}}$ and the user-defined threshold ϵ . The operation COMPUTE-ADMITTANCE in line 4-5 is performed via (1), and requires $O(l^3)$ computation, where l is the number of filaments. Assume that k iterations are needed for the **while** loop, which is dominated by the operation COMPUTE-ADMITTANCE, the total complexity of ADAPTIVE-MESHING is

$$O\left(\sum_{i=1}^k (i^2)^3\right) = O(k^7).$$

With i denoting the iteration index, the number of filaments are $(i+1)(i-1)$ and i^2 if i is even and odd, respectively. At termination, the number of filaments n is equal to k^2 in the worst case, and therefore the complexity of ADAPTIVE-MESHING is $O(n^{3.5})$. Assuming that there are m conductors, the overall complexity of our technique is $O(mn^{3.5})$. However, the complexity can be further reduced in several ways. First, we note that the discretization of a conductor depends only on its cross-section, and thus the run-time of the proposed adaptive meshing schemes is dependent only on the number of distinct cross-sections \hat{m} (and not the number of conductors m). Second, we can sort the distinct cross-sections in an increasing order before running the procedure ADAPTIVE-

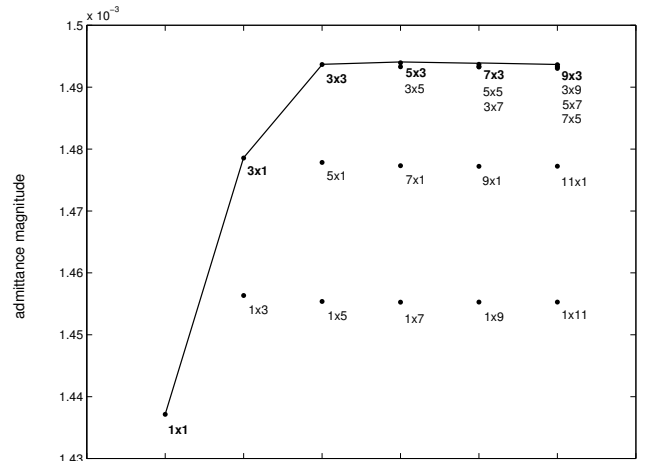


Fig. 10. Admittance values of a wire corresponding to the different discretizations in Fig. 9.

TABLE I
AN EXAMPLE OF THREE CONDUCTORS SHOWING THE NON-EFFECT OF PROXIMITY.

Mesh size	spacing (μm)									
	0.1		0.5		1.0		1.5		2.0	
	$ Y (\times 10^{-2})$	error	$ Y (\times 10^{-2})$	error	$ Y (\times 10^{-2})$	error	$ Y (\times 10^{-2})$	error	$ Y (\times 10^{-2})$	error
5×3	2.5094	0.9793%	1.5437	0.8933%	1.1063	0.8442%	0.8973	0.8155%	0.7724	0.8188%
7×3	2.5166	0.8609%	1.5465	0.7788%	1.1078	0.7296%	0.8984	0.6995%	0.7732	0.8188%
5×5	2.5077	0.9375%	1.5421	0.8622%	1.1050	0.8196%	0.8962	0.7946%	0.7715	0.8188%
9×3	2.5176	0.8143%	1.5470	0.7425%	1.1082	0.6992%	0.8987	0.6720%	0.7734	0.8188%
7×5	2.5135	0.9400%	1.5440	0.8639%	1.1060	0.8209%	0.8970	0.7957%	0.7720	0.8188%

ADAPTIVE-MESHING($\mathcal{G}_{\text{initial}}, \epsilon$)

```

1  $Y_{\text{initial}} \leftarrow \text{COMPUTE-ADMITTANCE}(\mathcal{G}_{\text{initial}})$ 
2  $Y_{\text{parent}} \leftarrow Y_{\text{initial}}, Y_{\text{change}} \leftarrow Y_{\text{parent}}$ 
3 while  $Y_{\text{change}} > \epsilon$ 
4   do  $Y_{\text{right}} \leftarrow \text{COMPUTE-ADMITTANCE}(\mathcal{G}_{\text{right}})$ 
5      $Y_{\text{left}} \leftarrow \text{COMPUTE-ADMITTANCE}(\mathcal{G}_{\text{left}})$ 
6     if  $Y_{\text{right}} \geq Y_{\text{left}}$ 
7       then  $Y_{\text{change}} \leftarrow |Y_{\text{right}} - Y_{\text{parent}}|$ 
8          $\text{parent} \leftarrow \text{right child}$ 
9       else  $Y_{\text{change}} \leftarrow |Y_{\text{left}} - Y_{\text{parent}}|$ 
10         $\text{parent} \leftarrow \text{left child}$ 

```

Fig. 11. Implementation of Adaptive Meshing Schemes.

MESHING. Once the discretization for a smaller cross-section is determined, we can use it to initialize the algorithm for the discretization of the next (larger) cross-section. As a result, the number of iterations in ADAPTIVE-MESHING can be substantially reduced.

V. EXPERIMENTAL RESULTS

We present application of AEM schemes on two classes of problems in the analysis of VLSI interconnects. The first is one of simulation, and the second is on the frequency-dependent inductance extraction. Note that the run-times of AEM schemes throughout this section include not only the simulation and extraction times but also the pre-processing time for determining the discretizations.

A. Simulation of wires of uniform cross-section

Consider an example of five parallel conductors of size of $3 \times 1 \times 1000\mu\text{m}$ each, with an inter-conductor separation of $1\mu\text{m}$. Both AEM-1 and AEM-2 applied with a threshold of 10^{-6} for the change in the admittance magnitude yield a discretization of 5×3 for the conductors. The center conductor is taken as the victim, with the four aggressors (two on each side) triggered by a ramp signal with a rise-time of 10ps. Owing to the enormous computational demands of SPICE, the simulation of only one input pattern is shown. Table II lists the discretizations, relative simulation errors and run-times for the various meshing schemes. The simulation arising from the UM (15×5 grid) is taken as the standard. It is evident from Table II that the runtime arising from discretizations suggested by the AEM schemes is only 0.066 times that of EM, with a negligible loss in accuracy.

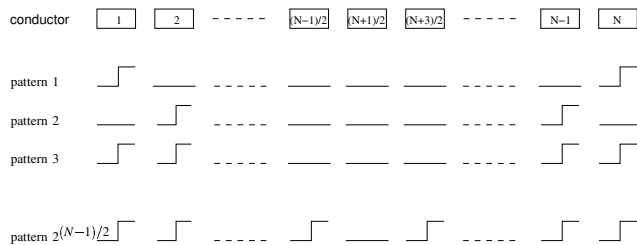


Fig. 12. Input patterns of simulation.

Second, we consider N conductors in parallel, each with a cross-section of $5 \times 1\mu\text{m}$ and length $1000\mu\text{m}$, with an inter-conductor spacing of $1\mu\text{m}$. As SPICE simulation is impractical, a fast simulator (from [2]) is used for the simulations. The center conductor is taken as the victim, and the aggressor inputs are ramp signals with a rise-time of 10ps. For simplicity, the aggressor switching patterns are assumed to be symmetric with respect to the victim, and a total of $2^{(N-1)/2}$ switching patterns are simulated (see Fig 12). The simulation arising from the UM discretization (25×5 grid) is taken as the standard, and the relative simulation errors, averaged over all conductors and switching patterns, are listed in Table III. The table also lists the run-times arising from discretizations suggested by different meshing schemes, normalized with respect to those of the EM-1 scheme. The conclusion is that compared to the simulation result of EM, the error of AEM is within 1% of UM and the speed-up is as high as $3 \times$.

B. Simulation of wires of non-uniform cross-sections

Typical VLSI interconnects have non-uniform cross-sections. Here, we consider an example of five parallel conductors and an example of seven parallel conductors. In both examples, the length and height of each conductor are 1mm and $3\mu\text{m}$, respectively. The widths are randomly chosen from the set $\{3\mu\text{m}, 5\mu\text{m}, 7\mu\text{m}\}$. As before, the center conductor is taken as the victim, the aggressor inputs are ramp signals with a rise-time of 10ps, and the aggressor switching patterns are assumed to be symmetric with respect to the victim. The sim-

TABLE II
A SMALL EXAMPLE : 5 PARALLEL CONDUCTORS

meshing scheme	EM-1	EM-2	AEM-1	AEM-2	UM
discretization	7×4	7×4	5×3	5×3	15×5
simulation error	0.327%	0.174%	0.374%	0.542%	0.000%
Runtime (hour)	3.32	3.25	0.22	0.21	298.39

TABLE III
PERFORMANCE OF CIRCUIT SIMULATION FOR INTERCONNECTS WITH UNIFORM CROSS-SECTION.

number of conductors	discretization							
	EM-1		EM-2		AEM-1		AEM-2	
	8 × 4		8 × 4		5 × 3		5 × 3	
N	error	runtime	error	runtime	error	runtime	error	runtime
5	0.1492%	1.00	0.1101%	1.07	0.5936%	0.67	0.5346%	0.67
7	0.1571%	1.00	0.1160%	1.07	0.6835%	0.58	0.5742%	0.60
9	0.1581%	1.00	0.1183%	1.03	0.7202%	0.44	0.5841%	0.44
11	0.1576%	1.00	0.1184%	1.01	0.8279%	0.29	0.5865%	0.29
13	0.1635%	1.00	0.1231%	0.97	1.0085%	0.35	0.5993%	0.35

TABLE IV
PERFORMANCE OF CIRCUIT SIMULATION FOR INTERCONNECTS WITH VARIOUS CROSS-SECTIONS.

number of conductors	EM-1		EM-2		AEM-1		AEM-2	
N	error	runtime	error	runtime	error	runtime	error	runtime
5	0.2121%	1.00	0.1263%	1.04	0.5682%	0.42	0.8481%	0.44
7	0.2133%	1.00	0.1311%	1.07	0.5521%	0.14	0.7421%	0.14

ulation arising from the UM discretization (15×15 , 25×15 , and 35×15 grids for $3\mu\text{m} \times 3\mu\text{m}$, $5\mu\text{m} \times 3\mu\text{m}$, and $7\mu\text{m} \times 3\mu\text{m}$ cross-sections, respectively) is taken as the standard, and the average relative simulation errors and normalized run-times are listed in Table IV. Compared to the simulation result of EM, the error of AEM is within 0.8% of UM, and the speed-up is as high as $7\times$.

Note that in general, signals in real circuits have multiple frequency components. For the purpose of determining a discretization that is appropriate for a conductor over a frequency range, we use the highest frequency of signals for determining the discretization.

C. Extraction of frequency-dependent inductance

We have also successfully applied the AEM schemes to speed-up the extraction of frequency-dependent inductance (or in general, frequency-dependent impedance) with little loss in accuracy. In this experiment, we consider a *spiral inductor* composed of segments with a uniform cross-section of $3\mu\text{m} \times 1\mu\text{m}$. The longest segment is $20\mu\text{m}$ long and the separation between any pair of adjacent parallel segments is $1\mu\text{m}$. The underlying algorithm used for the extraction of frequency-dependent inductance is FastHenry [3]. The discretizations determined using the UM, EM, and AEM schemes over a set of frequency points taken from the 10GHz–100GHz range are used by FastHenry for the frequency-dependent inductance extraction. For EM-1, AEM-1, and AEM-2, the respective discretizations at each frequency point are determined as outlined in §II and §IV. For EM-2, the discretization at each frequency point is determined based on the number of filaments used in a corresponding EM-1 discretization. For UM, which is again taken to be the standard, we use the coarsest uniform discretization where the width and the height of each filament are no larger than the skin depth δ . Table V lists the relative errors, averaged over all frequency points, and the total run-times arising from different discretization schemes. Compared to the result of EM, the error of AEM is within 0.6% of UM and the speed-up is as high as $3\times$.

TABLE V
PERFORMANCE OF INDUCTANCE EXTRACTION FOR SPIRAL INDUCTOR.

meshing scheme	EM-1	EM-2	AEM-1	AEM-2
error	0.0913%	0.0885%	0.6063%	0.1726%
runtime(second)	12.60	12.33	4.01	7.60
speedup	1.00	1.02	3.14	1.66

VI. CONCLUSION

We have presented a new adaptive algorithm for discretizing interconnects to account for high-frequency effects. The algorithm uses an easily-computable quantity that correlates well with simulation errors that arise from discretizations; this quantity is used in an adaptive meshing scheme to determine the coarsest discretization of conductors that provides an acceptable model accuracy, thus obtaining the maximum possible reduction in computation time. Experimental results demonstrate that the proposed adaptive meshing schemes yield a significant speed-up in inductance extraction and interconnect simulation with little sacrifice in accuracy.

REFERENCES

- [1] C. Cheng, J. Lillis, S. Lin, and N. Chang. *Interconnect Analysis and Synthesis*. John-Wiley, 2000.
- [2] J. Jain, C.-K. Koh, and V. Balakrishnan. Fast simulation of VLSI interconnects. In *Proc. Int. Conf. on Computer Aided Design*, pages 93–98, 2004.
- [3] M. Kamon, M. J. Tsuk, and J. K. White. FASTHENRY: A multipole-accelerated 3-D inductance extraction program. *IEEE Journal on Microwave Theory and Techniques*, 42(9):1750–1758, Sept. 1994.
- [4] T. Makkonen, V. P. Plessky, S. Kondratiev, and M. M. Salomaa. Electromagnetic modeling of package parasitics in SAW-duplexer. In *Proc. IEEE Ultrasonics Symposium*, pages 29–32, 1996.